Headline Articles

Isolation and Structural Characterization of Complexes Formed in the Reactions of $[\{C_5H_4(SiMe_3)\}_2Fe_2(CO)_4]$ and $[\{1,3\text{-}C_5H_3(SiMe_3)_2\}_2Fe_2(CO)_4]$ with Elemental Sulfur

Mikiya Yamada, Hiromi Tobita, Shinji Inomata, and Hiroshi Ogino*

Department of Chemistry, Graduate School of Science, Tohoku University, Sendai 980-77

(Received December 4, 1995)

The reactions of $[Cp^{S1}{}_2Fe_2(CO)_4]$ and $[Cp^{S2}{}_2Fe_2(CO)_4]$ with elemental sulfur afforded a tetrairon cluster containing two end-on type S_2 ligands $[Cp^{S1}{}_4Fe_4S_6]$ (**1**) and a diiron complex containing an end-on type S_2 and a side-on type S_2 ligands $[Cp^{S2}{}_2Fe_2S_4]$ (**2**), respectively, where Cp^{S1} and Cp^{S2} stand for mono- and bis(trimethylsilyl)cyclopentadienyl ligands, respectively. From these results and the previously reported results which were obtained for the reactions of $[Cp_2Fe_2(CO)_4]$ and $[Cp^*{}_2Fe_2(CO)_4]$ with elemental sulfur, it is suggested that $[Cp'{}_2Fe_2S_4]$ is an intermediate to give tetrairon sulfur clusters, where Cp^* and Cp' denote pentamethylcyclopentadienyl and substituted cyclopentadienyl ligands, respectively. X-Ray crystal structure analysis was carried out for the compounds **1** and **2**. Crystallographic data are as follows: **1**: Monoclinic, $P2_1/c$, $a=17.302(6)$, $b=18.646(3)$, $c=15.310(4)$ Å, $\beta=120.71(2)°$, $V=4246(2)$ Å^3, $Z=4$, and $R=0.061$ for 5850 reflections with $|F_o|>3\sigma(F_o)$; **2**: Triclinic, space group $P\bar{1}$, $a=12.602(2)$, $b=12.891(2)$, $c=11.401(1)$ Å, $\alpha=114.52(1)$, $\beta=95.45(1)$, $\gamma=88.39(1)°$, $V=1677.5(4)$ Å^3, $Z=2$, and $R=0.046$ for 7343 reflections with $|F_o|>3\sigma(F_o)$.

Reaction of $[Cp^*{}_2Fe_2(CO)_4]$ with elemental sulfur gives a diiron complex $[Cp^*{}_2Fe_2S_4]$ with a bidentate and a doubly bidentate μ-S_2 ligands in a good yield (Eq. 1).[1,2]

$$[Cp^*{}_2Fe_2(CO)_4] + \frac{1}{2}S_8 \xrightarrow[\text{reflux}]{\text{toluene}} [Cp^*{}_2Fe_2S_4] \quad (1)$$

However, if $[Cp_2Fe_2(CO)_4]$ is used in place of $[Cp^*{}_2Fe_2(CO)_4]$, a mixture of tetrairon clusters is obtained as major products (Eq. 2).[3—5]

$$2[Cp_2Fe_2(CO)_4] + \frac{n}{8}S_8 \xrightarrow[\text{reflux}]{\text{toluene}} [Cp_4Fe_4S_n] \ (n=4,5,6) \quad (2)$$

$[Cp_4Fe_4S_4]$ has a cubane structure. $[Cp_4Fe_4S_5]$ and $[Cp_4Fe_4S_6]$ contain one and two disulfide ligands, respectively. The difference of the products mentioned above likely results from that of the bulkiness of Cp and Cp^* ligands. In order to confirm this, using Cp^{S1} and Cp^{S2} which contain bulky trimethylsilyl group(s), the products of the reactions of $[Cp^{S1}{}_2Fe_2(CO)_4]$ and $[Cp^{S2}{}_2Fe_2(CO)_4]$ with elemental sulfur were isolated and characterized.

Experimental

All manipulations were carried out under inert atmosphere using standard Schlenk techniques. All solvents were dried and deoxygenated by standard methods. $C_5H_5(SiMe_3)$ (HCp^{S1}),[6] 1,1-$C_5H_4(SiMe_3)_2$ (HCp^{S2}),[7] $[Cp^{S1}{}_2Fe_2(CO)_4]$,[8] and $[Cp^{S2}{}_2Fe_2(CO)_4]$[9] were prepared as reported in the literature.

^{1}H NMR spectra were recorded on JEOL FX-90Q, Varian XL-200, and Bruker ARX 300 spectrometers. ^{13}C and ^{29}Si NMR spectra were recorded on the JEOL FX-90Q and the Bruker ARX 300 spectrometers, IR spectra on a JASCO IR-810 spectrophotometer, UV-vis spectra on a Shimadzu UV 260 spectrophotometer, and mass spectra on a JEOL JMS-HX110 spectrometer.

Cyclic voltammetry was carried out with a Fuso Model 311 potentiostat and a Model 321 function generator. Measurements were made in 0.1 M (1 M=1 mol dm^{-3}) tetrabutylammonium tetrafluoroborate (TBAB)/acetonitrile solutions with a three-electrode system with a platinum rod working electrode, a platinum coil auxiliary electrode, and a saturated calomel reference electrode (SCE). A sample solution was coupled through a salt bridge filled with a 0.1 M TBAB solution to the reference electrode.

$[Cp^{S1}{}_4Fe_4S_6]$ (1). A solution of $[Cp^{S1}{}_2Fe_2(CO)_4]$ (501 mg, 1.01 mmol) and elemental sulfur (121 mg, 0.47 mmol) in toluene (40 mL) was heated at 90 °C for 20 h with stirring. After removal of a black precipitate (137 mg) by filtration, toluene was evaporated under reduced pressure. The residue was subjected to silica gel flash chromatography (column size: 3.5×24 cm). Three bands were eluted by toluene/diethyl ether. Evaporation of the solvent from the first fraction afforded black flakes. Spectroscopic data suggest that the compound is $[Cp^{S1}{}_4Fe_4S_5]$. Yield 44 mg (9%). Data for the compound: ^{1}H NMR (C_6D_6, 90 MHz) $\delta=0.44$ (br, 36H, $SiMe_3$),

3.98 (br, 8H, $C_5H_4SiMe_3$), 4.40 (br, 8H, $C_5H_4SiMe_3$); MS (FAB, *m*-nitrobenzyl alcohol matrix, Xe) *m/z* (% rel intensity) 932 (M^+; 100), 900 ($[Cp^{S1}{}_4Fe_4S_4]^+$; 16).

After removal of the solvent from the second fraction, $[Cp^{S1}{}_4Fe_4S_6]$ (**1**) was obtained as black flakes. Yield 201 mg (42%). Data for **1**: ^{1}H NMR (toluene-d_8, 300 MHz) δ=0.41 (s, 18H, $SiMe_3$), 0.54 (s, 18H, $SiMe_3$), 2.74 (bs, 2H, H_β), 3.08 (bs, 2H, H_β), 3.18 (bs, 2H, H_α), 3.30 (bs, 2H, H_α), 4.34 (br, 2H, H_β), 4.81 (bs, 2H, H_α), 5.58 (bs, 2H, H_β), 6.16 (bs, 2H, H_α); ^{13}C NMR (toluene-d_8, 75.5 MHz, −43 °C) δ=−0.01, 0.04 ($SiMe_3$), 85.4, 86.4, 86.8, 88.1, 88.7, 89.1, 89.47, 89.54, 99.8, 102.8 ($C_5H_4SiMe_3$); ^{29}Si NMR (toluene-d_8, 59.6 MHz) δ=−2.92, −2.73 ($SiMe_3$); IR (KBr pellet) 1246 s (δ_{Si-Me}), 509 w (ν_{S-S}), 415 w (ν_{Fe-S}) cm^{-1}; MS (FAB, *m*-nitrobenzyl alcohol matrix, Xe) *m/z* (% rel intensity) 964 (M^+; 100), 932 ($[Cp^{S1}{}_4Fe_4S_5]^+$; 65), 900 ($[Cp^{S1}{}_4Fe_4S_4]^+$; 36), 827 ($[Cp^{S1}{}_3Fe_4S_6]^+$; 34), 795 ($[Cp^{S1}{}_3Fe_4S_5]^+$; 28), 763 ($[Cp^{S1}{}_3Fe_4S_4]^+$; 91); UV-vis (CH_3CN) λ_{max} (ε) 349sh (7200), 260 (23000) nm. Anal. Found: C, 39.84; H, 5.43%. Calcd for $C_{32}H_{52}Fe_4S_6Si_4$: C, 39.85; H, 5.35%.

Evaporation of the solvent from the third fraction afforded a brown oil which was not identified.

When a solution of $[Cp^{S1}{}_2Fe_2(CO)_4]$ (201 mg, 0.40 mmol) and sulfur (55 mg, 0.21 mmol) in toluene (16 mL) was heated at 100 °C for shorter time (2h), 49 mg of **1** was obtained after the same workup as mentioned above. Yield 26%. Chromatographic separation afforded four fractions including that of **1** as the third fraction. Evaporation of the solvent from the second fraction afforded a brown powder which was identified as $[Cp^{S1}{}_2Fe_2S_4]$ from spectroscopic data. Yield 10 mg (5%). Data for $[Cp^{S1}{}_2Fe_2S_4]$: ^{1}H NMR (C_6D_6, 90 MHz) δ=0.07 (s, 18H, $SiMe_3$), 4.60 (m, 4H, H_β), 5.16 (m, 4H, H_α); IR (KBr pellet) 1244 s (δ_{Si-Me}); 534 w (ν_{S-S}); 458 w, 418 w (ν_{Fe-S}) cm^{-1}; UV-vis (CH_3CN) λ_{max} (ε) 784 (4500), 474 (5400), 275 (13000) nm; MS (FAB, *m*-nitrobenzyl alcohol matrix, Xe) *m/z* (% rel intensity) 514 (M^+; 20), 482 ($[Cp^{S1}{}_2Fe_2S_3]^+$; 16), 450 ($[Cp^{S1}{}_2Fe_2S_2]^+$; 51).

$[Cp^{S2}{}_2Fe_2S_4]$ (2). A solution of $[Cp^{S2}{}_2Fe_2(CO)_4]$ (1.97 g, 3.07 mmol) and elemental sulfur (410 mg, 1.60 mmol) in toluene (30 mL) was heated at 100 °C for 20 h with stirring. After removal of a black precipitate (38 mg) by filtration, toluene was evaporated under reduced pressure and the residue was subjected to silica gel flash chromatography (column size: 3.5×29 cm). Two bands were eluted by hexane/toluene (10 : 1). Evaporation of the solvent from the first fraction afforded the known complex $[Cp^{S2}{}_2Fe]$.[10] Yield 14 mg (1%). Evaporation of the solvent from the second fraction afforded $[Cp^{S2}{}_2Fe_2S_4]$ (**2**) as a dark reddish brown powder. Yield 1.46 g (72%). Data for **2**: ^{1}H NMR (C_6D_6, 90 MHz) δ=0.01 (s, 36H, $SiMe_3$), 4.87 (bs, 4H, $C_5H_3(SiMe_3)_2$), 6.07 (bs, 2H, $C_5H_3(SiMe_3)_2$); ^{13}C NMR (C_6D_6, 22.5 MHz) δ=−0.10 ($SiMe_3$), 83.0, 92.0 ($C_5H_3(SiMe_3)_2$); IR (KBr pellet) 1249 s (δ_{Si-Me}), 536 w (ν_{S-S}), 410 w (ν_{Fe-S}) cm^{-1}; UV-vis (hexane) λ_{max} (ε) 787 (3640), 474 (4720), 325sh (12500), 279 (29000) nm; MS (EI, 16.5 eV, 100 °C) *m/z* (% rel intensity) 658 (M^+; 32), 594 ($[Cp^{S2}{}_2Fe_2S_2]^+$; 62), 449 ($[Cp^{S2}Fe_2S_4]$; 45). Anal. Found: C, 40.07; H, 6.60%. Calcd for $C_{22}H_{42}Fe_2S_4Si_4$: C, 40.11; H, 6.43%.

X-Ray Crystal Structural Determination of $[Cp^{S1}{}_4Fe_4S_6]$ (1) and $[Cp^{S2}{}_2Fe_2S_4]$ (2). Crystals of **1** suitable for X-ray analysis were grown by gradually cooling the pentane solution from room temperature to −80 °C. Crystals of **2** suitable for X-ray analysis were obtained by layering a dichloromethane solution of **2** with ethanol.

Diffraction data for **1** and **2** were collected on a Rigaku AFC-6A four-circle diffractometer with graphite-monochromated Mo $K\alpha$ radiation using the ω–2θ scan technique. Crystallographic data for **1** and **2** are listed in Table 1. The reflection data were corrected for Lorentz and polarization factors. No correction was applied for absorption. The unit cell dimensions were determined by the least-squares method using 75 reflections in the range of $25° < 2\theta < 30°$ for **1** and 25 reflections in the range of $30° < 2\theta < 35°$ for **2**.

The structures of **1** and **2** were solved by the direct method (MULTAN) and the heavy atom method, respectively. The parameters were refined by the block-diagonal least-squares method. Anisotropic temperature factors were applied for the non-hydrogen atoms. The positions of the hydrogen atoms except for those of the hydrogen atoms on trimethylsilyl groups were deduced from the difference Fourier map, and isotropically refined.

Values for the atomic scattering factors of non-hydrogen and hydrogen atoms were those in Refs. 11 and 12, respectively. Calculations were performed on a Nippon Electric Co. ACOS-1000 computer at Tohoku University Computer Center using the Universal Computation Program System UNICS III.[13] The tables of the bond distances and angles, the anisotropic temperature factors for non-hydrogen atoms, the atomic coordinates for hydrogen atoms, and the $F_o - F_c$ are deposited as Document No. 69019 at the Office of the Editor of Bull. Chem. Soc. Jpn.

Results and Discussion

Isolation and Characterization of Reaction Products. Reaction of $[Cp^{S1}{}_2Fe_2(CO)_4]$ with sulfur in toluene at 90 °C for 20 h afforded $[Cp^{S1}{}_4Fe_4S_6]$ (**1**), $[Cp^{S1}{}_4Fe_4S_5]$, and $[Cp^{S1}{}_2Fe_2S_4]$. The spectroscopic data for the compounds show that the structural assignments are reasonable, but effective purification could not be performed for the latter two compounds so that we cannot offer satisfactory results of

Table 1. Crystallographic Data for $[Cp^{S1}{}_4Fe_4S_6]$ (**1**) and $[Cp^{S2}{}_2Fe_2S_4]$ (**2**)

	1	**2**
Formula	$C_{32}H_{52}Fe_4S_6Si_4$	$C_{22}H_{42}Fe_2Si_4S_4$
Formula weight	964.86	658.85
Crystal system	Monoclinic	Triclinic
Space group	$P2_1/c$	$P\bar{1}$
a/Å	17.302(6)	12.602(2)
b/Å	18.646(3)	12.891(2)
c/Å	15.310(4)	11.401(1)
α/°		114.52(1)
β/°	120.71(2)	95.45(1)
γ/°		88.39(1)
V/Å^3	4246(2)	1677.5(4)
Z	4	2
Radiation (Mo $K\alpha$)/Å	0.71073	0.71073
T/°C	20	20
D_{calcd}/g cm^{-3}	1.526	1.304
μ(Mo$K\alpha$)/cm^{-1}	17.6	12.6
No. of reflcns measd	10047	9830
No. of reflcns used ($\|F_o\| > 3\sigma(F_o)$)	5850	7343
R[a]	0.061	0.046
R_w[b]	0.087	0.094

a) $R = \Sigma\|\|F_o\| - \|F_c\|\|/\Sigma|F_o|$. b) $R_w = [\Sigma w(|F_o| - |F_c|)^2 / \Sigma w|F_o|^2]^{1/2}$; $w = [\sigma^2(|F_o|) + aF_o{}^2]^{-1}$, where a=0.005 for **1** and 0.015 for **2**.

elemental analysis.

The ^{1}H NMR spectrum of **1** shows two singlets assignable to the $SiMe_3$ groups and eight signals assignable to the ring protons on Cp^{S1} ligands (Fig. 1). The spectral pattern is consistent with the X-ray crystal structure (vide infra). The cluster **1** has two kinds of Cp^{S1} ligands with magnetically different environments and the cluster core is chiral. Therefore each pair of α protons and β protons with respect to the $SiMe_3$ group in a Cp^{S1} ligand is diastereotopic, so that four ring protons on the Cp^{S1} ligand become all non-equivalent. As a whole, the molecule has eight magnetically different ring protons. The elemental analysis, ^{13}C and ^{29}Si NMR spectral data, and FAB MS data also support the molecular structure.

When a toluene solution containing $[Cp^{S1}{}_2Fe_2(CO)_4]$ and sulfur was heated at 100 °C for a short time (2 h), formation of a small amount of $[Cp^{S1}{}_2Fe_2S_4]$ was observed. This suggests that $[Cp^{S1}{}_2Fe_2S_4]$ is an intermediate to tetrairon–sulfur clusters $[Cp^{S1}{}_2Fe_2S_5]$ and $[Cp^{S1}{}_4Fe_4S_6]$.

The reaction of $[Cp^{S2}{}_2Fe_2(CO)_4]$ with sulfur yielded $[Cp^{S2}{}_2Fe_2S_4]$ (**2**) in a good yield and no tetrairon cluster was detected. Spectroscopic data for **2** were consistent with the formulation $[Cp^{S2}{}_2Fe_2S_4]$: The IR spectrum of **2** shows Si–Me deformation at 1249 cm^{-1}. The ^{1}H NMR spectrum shows a singlet for the trimethylsilyl group at δ=0.01 ppm and two singlets for the cyclopentadienyl ring protons at δ=4.87 and 6.07 ppm with the intensity ratio of 2 : 1. This means that there is only one kind of Cp^{S2} in the molecule. The UV-vis spectrum shows two absorption maxima at 787 and 474 nm with a spectral pattern quite similar to that of $[Cp^*{}_2Fe_2S_4]$.[14] The elemental analysis and ^{13}C NMR and FAB Mass spectral data also support the formulation.

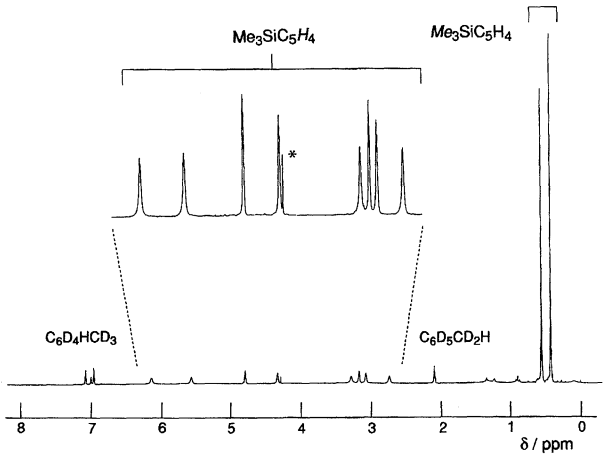

Fig. 1. ^{1}H NMR spectrum (300 MHz, toluene-d_8) of $[Cp^{S1}{}_4Fe_4S_6]$ (**1**) at room temperature (asterisk represents impurity).

The reactions of $[Cp'{}_2Fe_2(CO)_4]$ (Cp′=Cp, Cp^{S1}, Cp^{S2}, Cp^*) with sulfur can be summarized as shown in Scheme 1. The reactions of $[Cp'{}_2Fe_2(CO)_4]$ containing bulky Cp′ ligands give diiron–sulfur complexes, while those containing less bulky Cp′ ligands afford tetrairon–sulfur clusters. $[Cp^{S1}{}_2Fe_2(CO)_4]$ is a border line compound which reacts with sulfur to yield the tetrairon–sulfur clusters and the diiron–sulfur compound.

Electrochemical Properties of 1 and 2. Cyclic voltammetric data of **1**, **2**, and related compounds are summarized in Table 2. Tetrairon cluster $[Cp^{S1}{}_4Fe_4S_6]$ (**1**) shows three redox processes which are composed of two reversible one-electron oxidation waves and a quasi-reversible two-electron reduction wave. The electrochemical behavior of the reduction wave is different from that of related clusters $[Cp_4Fe_4S_6]$[5,16] and $[(MeCp)_4Fe_4S_6]$.[1,17] Each of the latter two clusters also gives three redox waves. However, the reduction wave does not correspond to a two-electron process, but to a one-electron process, though we can not offer an explanation for the difference.

The redox potentials of **1** have more negative values than those of $[Cp_4Fe_4S_6]$ and $[(MeCp)_4Fe_4S_6]$. This is caused by the trimethylsilyl group on the cyclopentadienyl ligand which makes the Cp^{S1} ligand more electron-donating than the Cp ligand. However, the negative shift of the redox potentials of **1** is not large, since the Cp^{S1} ligand can also act as a better π-electron acceptor than Cp.

Diiron complex $[Cp^{S2}{}_2Fe_2S_4]$ (**2**) gives a reversible one-electron oxidation wave and a quasi-reversible one-electron reduction wave. This electrochemical pattern is the same as that of $[Cp^*{}_2Fe_2S_4]$.[18] Two isomers have been known for $[Cp_2Fe_2S_4]$, IA and IB.[19] X-Ray crystallography revealed that the former isomer has approximate C_{2v} symmetry with two bridging disulfide ligands.[19b] However, the structure of the latter isomer is still uncertain. Each of them exhibits an irreversible oxidation wave and an irreversible two-electron reduction wave. The redox potentials of **2** shift to more positive ranges than those of $[Cp^*{}_2Fe_2S_4]$. This indicates that Cp^* is more electron-donating than Cp^{S2}. It should be also noted, however, that Cp^{S2} has compensating effects: Cp^{S2} is simultaneously a stronger electron-donor and a better π-acceptor than Cp^* ligand.

Structure of $[Cp^{S1}{}_4Fe_4S_6]$ (1). Four clusters have been reported as $[Cp'{}_4Fe_4S_6]$ type clusters; $[Cp_4Co_4S_6]$,[20] $[Cp_4Fe_4S_6]$,[4,5,21] $[(MeCp)_4Fe_4S_6]$,[17]

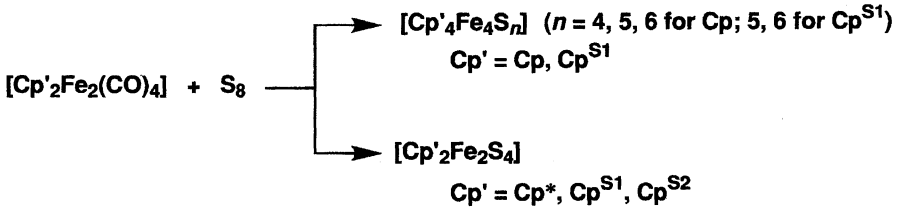

Scheme 1.

Table 2. Cyclic Voltammetric Data of $[Cp^{S1}{}_4Fe_4S_6]$ (**1**), $[Cp^{S2}{}_2Fe_2S_4]$ (**2**), and Related Compounds[a)]

Redox couple	E_{pa}/V	E_{pc}/V	$E_{1/2}$/V	ΔE_p/mV	Supporting electrolyte–Solvent	Reference
$[\mathbf{1}]^{2+}/[\mathbf{1}]^{+}$	+0.29	+0.23	+0.26	60	0.1 M TBAB–CH_3CN[b)]	c)
$[\mathbf{1}]^{+}/[\mathbf{1}]$	−0.06	−0.12	−0.08	80		
$[\mathbf{1}]/[\mathbf{1}]^{2-}$	−1.24	−1.38	−1.31	140		
$[Cp_4Fe_4S_6]^{2+}/[Cp_4Fe_4S_6]^{+}$	—	—	+0.367	d)	0.1 M Bu_4NSbF_6–CH_2Cl_2[e)]	Ref. 5
$[Cp_4Fe_4S_6]^{+}/[Cp_4Fe_4S_6]$	—	—	+0.06	f)		
$[Cp_4Fe_4S_6]/[Cp_4Fe_4S_6]^{-}$	—	—	−1.325	f)		
$[Cp_4Fe_4S_6]^{2+}/[Cp_4Fe_4S_6]^{+}$	—	—	+0.34	d)	0.1 M Bu_4NPF_6–CH_2Cl_2[g,h)]	Ref. 16
$[Cp_4Fe_4S_6]^{+}/[Cp_4Fe_4S_6]$	—	—	+0.03	f)		
$[Cp_4Fe_4S_6]/[Cp_4Fe_4S_6]^{-}$	—	—	−1.24	f)		
$[(MeCp)_4Fe_4S_6]^{2+}/[(MeCp)_4Fe_4S_6]^{+}$	—	—	+0.24	f)	0.1 M Bu_4NPF_6–CH_2Cl_2[h)]	Ref. 17
$[(MeCp)_4Fe_4S_6]^{+}/[(MeCp)_4Fe_4S_6]$	—	—	−0.09			
$[(MeCp)_4Fe_4S_6]/[(MeCp)_4Fe_4S_6]^{-}$	—	—	−1.41			
$[\mathbf{2}]^{+}/[\mathbf{2}]$	+0.56	+0.49	+0.53	70	0.1 M TBAB–CH_3CN[b)]	c)
$[\mathbf{2}]/[\mathbf{2}]^{-}$	−1.14	−1.25	−1.20	110		
$[Cp^*{}_2Fe_2S_4]^{+}/[Cp^*{}_2Fe_2S_4]$	+0.30	+0.19	+0.25	100	0.1 M TBAB–CH_3CN[b)]	Ref. 18[i)]
$[Cp^*{}_2Fe_2S_4]/[Cp^*{}_2Fe_2S_4]^{-}$	−1.30	−1.39	−1.35	100		
$[Cp_2Fe_2S_4]$ (two isomers IA and IB)						
$[IA]^{+}/[IA]$	+0.56	—	—	e)	0.1 M TBAB–CH_3CN[g)]	Ref. 19
$[IA]/[IA]^{2-}$	—	−1.18	—	e)		
$[IB]^{+}/[IB]$	+0.66	—	—	e)	0.1 M TBAB–CH_3CN[f)]	Ref. 19
$[IB]/[IB]^{2-}$	—	−1.20	—	e)		

a) E_{pa}: anodic peak potential. E_{pc}: cathodic peak potential. $E_{1/2}$: half-wave potential. ΔE_p: $|E_{pa}-E_{pc}|$. Potentials are given in V vs. SCE. b) Sweep rate: 50 mV s^{-1}. c) This work. d) Quasi-reversible. e) Sweep rate: 200 mV s^{-1}. f) Reversible. g) Sweep rate: 100 mV s^{-1}. h) Potentials (V vs. ferrocene/ferricinium couple) given in Ref. 16 are converted into values in V vs. SCE by use of $E_{1/2}(Fc/Fc^+)$=+0.48 V vs. SCE. i) Data are taken from Ref. 18a.

and $[(EtCp^*)_4Ru_4S_6]$.[1,22)] Among them, the structures of $[Cp_4Co_4S_6]$ and $[Cp_4Fe_4S_6]$ have been determined by X-ray crystallography. Each M_4S_6 core of the clusters consists of four metal atoms, two μ_3-S ligands, and two "end-on" type μ_3-S_2 ligands. However, the structures differ considerably. The cobalt cluster has no metal–metal bond and no symmetry element so that all four cobalt atoms in the cluster are non-equivalent. $[Cp_4Fe_4S_6]$ has two metal–metal bonds and a C_2 axis. Therefore, two pairs of CpFe units are equivalent.

The structure of **1** is shown in Fig. 2. Final atomic coordinates and selected interatomic distances and angles are listed in Tables 3 and 4, respectively. The cluster **1** has an Fe_4S_6 core surrounded by four Cp^{S1} ligands. The structure of the core is almost identical with that of the Cp analogue $Cp_4Fe_4S_6$.[4,5,21)] The cluster **1** adopts approximate C_2 symmetry and is chiral, which is consistent with the ^1H NMR spectrum.

Bulky $SiMe_3$ groups on Cp^{S1} ligands are oriented to reduce their mutual steric repulsion: Two Cp^{S1} ligands ($Cp^{S1}(2)$, $Cp^{S1}(4)$) attached to Fe(2) and Fe(4) adopt *anti* conformation. On the other hand, the remaining two Cp^{S1} ligands ($Cp^{S1}(1)$, $Cp^{S1}(3)$) attached to Fe(1) and Fe(3) adopt *gauch* conformation.

The cluster **1** has two Fe–Fe bonds as seen for $[Cp_4Fe_4S_6]$:

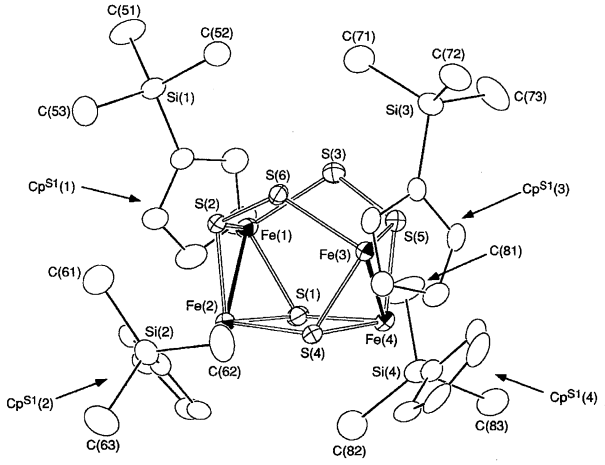

Fig. 2. ORTEP drawing of $[Cp^{S1}{}_4Fe_4S_6]$ (**1**).

The Fe(1)–Fe(2) and Fe(3)–Fe(4) distances are 2.667(2) and 2.653(2) Å, respectively, and are in the range expected for Fe–Fe single bonds. The remaining four Fe–Fe distances are very long (3.448(2)—4.365(2) Å), indicating the absence of Fe–Fe bonds. As given in Table 5, some of distances between methyl groups on the Cp^{S1} ligand and sulfur atoms in the Fe_4S_6 core are shorter than the sum of van der Waals radii

Table 3. Final Atomic Coordinates ($\times 10^4$) and Equivalent Isotropic Temperature Factors (Å^2) for [$Cp^{S1}{}_4Fe_4S_6$] (**1**)

Atom	x	y	z	B_{eq}[a)]
Fe(1)	2482.4(7)	4897.4(6)	6528.7(8)	2.9
Fe(2)	4066.1(6)	5526.5(6)	7161.5(7)	2.8
Fe(3)	2547.5(6)	7048.9(5)	5445.0(7)	2.6
Fe(4)	2863.6(7)	5928.0(6)	4605.0(7)	2.9
S(1)	3193.7(12)	4996.9(10)	5680.8(13)	3.0
S(2)	3028.7(11)	5870.6(9)	7478.8(12)	2.6
S(3)	1260.8(12)	5459.2(11)	5288.5(14)	3.3
S(4)	3812.9(11)	6438.9(10)	6064.9(13)	2.9
S(5)	1605.9(12)	6180.1(10)	4553.0(13)	3.0
S(6)	2494.4(12)	6838.4(10)	6858.8(13)	2.8
Si(1)	1518.4(15)	4898.4(12)	8155.6(17)	3.6
Si(2)	5557.6(15)	6801.3(14)	9059.7(18)	4.1
Si(3)	500.5(15)	8012.1(14)	4791.8(19)	4.2
Si(4)	2606.5(16)	4242.5(15)	3271.0(19)	4.3
C(11)	1989(5)	4421(4)	7441(6)	3.3
C(12)	1484(6)	4168(4)	6426(6)	3.8
C(13)	2056(7)	3818(5)	6165(7)	4.9
C(14)	2934(6)	3840(5)	7007(8)	4.7
C(15)	2891(5)	4220(4)	7793(6)	3.7
C(21)	5276(5)	5909(5)	8431(6)	3.7
C(22)	5440(5)	5646(5)	7652(6)	4.2
C(23)	5241(6)	4914(5)	7493(7)	4.7
C(24)	4941(5)	4693(5)	8145(7)	4.3
C(25)	4963(5)	5285(5)	8698(6)	3.9
C(31)	1659(5)	7932(4)	4973(5)	3.3
C(32)	1865(6)	7756(4)	4213(5)	3.6
C(33)	2783(6)	7831(4)	4582(6)	4.0
C(34)	3180(5)	8073(4)	5603(6)	3.6
C(35)	2501(5)	8138(4)	5835(5)	3.4
C(41)	2835(5)	5219(4)	3479(5)	3.5
C(42)	3678(6)	5574(5)	4044(6)	4.2
C(43)	3534(7)	6330(5)	3877(6)	4.9
C(44)	2625(8)	6447(5)	3234(7)	5.5
C(45)	2193(6)	5788(5)	2983(6)	4.7
C(51)	784(7)	4232(6)	8304(9)	5.9
C(52)	832(6)	5679(5)	7425(7)	5.0
C(53)	2469(6)	5178(5)	9431(7)	5.0
C(61)	5060(8)	6824(6)	9904(8)	6.2
C(62)	5089(8)	7562(5)	8119(7)	5.9
C(63)	6823(7)	6894(6)	9852(9)	6.3
C(71)	382(8)	7586(8)	5823(10)	8.0
C(72)	314(7)	9009(5)	4817(8)	5.5
C(73)	−305(7)	7593(6)	3537(9)	6.4
C(81)	1627(8)	4015(7)	3428(9)	7.5
C(82)	3651(7)	3729(6)	4157(8)	5.9
C(83)	2302(7)	4056(7)	1912(7)	6.3

a) The equivalent isotropic temperature factors for non-hydrogen atoms were computed using the following expression: $B_{eq}=4/3(B_{11}a^2+B_{22}b^2+B_{33}c^2+B_{13}ac\cos\beta)$. The B_{ij}'s are defined by $\exp[-(h^2B_{11}+k^2B_{22}+l^2B_{33}+2hkB_{12}+2hlB_{13}+2klB_{23})]$.

(3.8 Å) and indicate that severe steric crowding exists in the cluster. However, this does not give any significant influence on the Fe_4S_6 core. The twelve Fe–S bonding distances range from 2.182(3) to 2.270(3) Å, which are normal values for Fe–S single bonds.[4,21] The S–S bond distances of the two S_2 ligands are 2.029(2) and 2.029(4) Å which are comparable to those in the clusters and complexes containing S_2 ligands.[23]

Table 4. Selected Interatomic Distances (Å) and Angles (°) for [$Cp^{S1}{}_4Fe_4S_6$] (**1**)

Fe(1)–Fe(2)	2.667(2)	Fe(1)···Fe(3)	4.365(2)
Fe(1)···Fe(4)	3.845(2)	Fe(2)···Fe(3)	3.849(2)
Fe(2)···Fe(4)	3.448(2)	Fe(3)–Fe(4)	2.653(2)
Fe(1)–S(1)	2.206(3)	Fe(1)–S(2)	2.213(2)
Fe(1)–S(3)	2.252(2)	Fe(2)–S(1)	2.213(2)
Fe(2)–S(2)	2.182(3)	Fe(2)–S(4)	2.270(3)
Fe(3)–S(4)	2.206(2)	Fe(3)–S(5)	2.207(2)
Fe(3)–S(6)	2.247(3)	Fe(4)–S(1)	2.257(2)
Fe(4)–S(4)	2.203(2)	Fe(4)–S(5)	2.188(3)
S(2)–S(6)	2.029(2)	S(3)–S(5)	2.029(4)
S(1)–Fe(1)–S(2)	97.96(10)	S(1)–Fe(1)–S(3)	91.73(10)
S(2)–Fe(1)–S(3)	94.28(8)	S(1)–Fe(2)–S(2)	98.69(9)
S(1)–Fe(2)–S(4)	78.68(8)	S(2)–Fe(2)–S(4)	94.26(9)
S(4)–Fe(3)–S(5)	98.31(8)	S(4)–Fe(3)–S(6)	90.88(9)
S(5)–Fe(3)–S(6)	95.02(9)	S(1)–Fe(4)–S(4)	79.19(8)
S(1)–Fe(4)–S(5)	93.91(10)	S(4)–Fe(4)–S(5)	99.00(10)
Fe(1)–S(1)–Fe(2)	74.24(10)	Fe(1)–S(1)–Fe(4)	119.01(11)
Fe(2)–S(1)–Fe(4)	100.97(8)	Fe(1)–S(2)–Fe(2)	74.71(8)
Fe(1)–S(2)–S(6)	118.83(10)	Fe(2)–S(2)–S(6)	112.80(13)
Fe(1)–S(3)–S(5)	111.13(12)	Fe(2)–S(4)–Fe(3)	118.61(12)
Fe(2)–S(4)–Fe(4)	100.87(8)	Fe(3)–S(4)–Fe(4)	74.01(6)
Fe(3)–S(5)–Fe(4)	74.28(7)	Fe(3)–S(5)–S(3)	118.44(13)
Fe(4)–S(5)–S(3)	113.99(12)	Fe(3)–S(6)–S(2)	111.90(13)

Table 5. Interatomic Distances (Å) between Trimethylsilyl Carbon Atoms on Cp^{S1} and Sulfur Atoms in the Fe_4S_6 Core of [$Cp^{S1}{}_4Fe_4S_6$] (**1**)

S(1)···C(81)	3.613(13)	S(1)···C(82)	3.680(15)
S(2)···C(52)	3.777(13)	S(2)···C(53)	3.808(14)
S(3)···C(52)	3.728(16)	S(4)···C(62)	3.472(11)
S(5)···C(73)	3.877(11)	S(6)···C(71)	3.450(13)

Structure of [$Cp^{S2}{}_2Fe_2S_4$] (2). The structure of **2** is shown in Fig. 3. Final atomic coordinates and selected interatomic distances and angles are listed in Tables 6 and 7, respectively. Complex **2** has an Fe_2S_4 core with approximate C_{2v} symmetry. The structure of the Fe_2S_4 core is very similar to the Cp and Cp* analogues [$Cp_2Fe_2S_4$][19] and [$Cp^*{}_2Fe_2S_4$].[2] Each Fe_2S_4 core

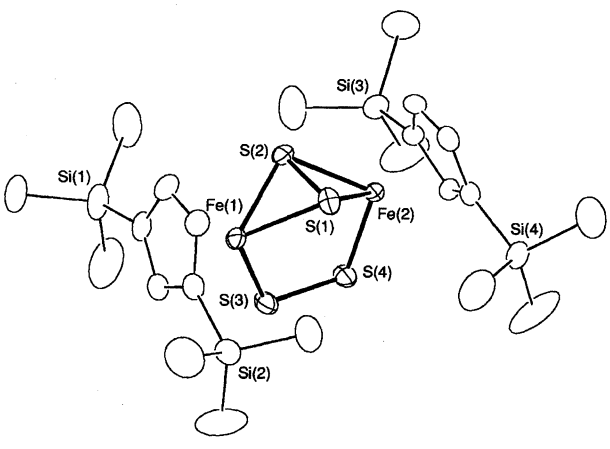

Fig. 3. ORTEP drawing of [$Cp^{S2}{}_2Fe_2S_4$] (**2**).

Table 6. Final Atomic Coordinates ($\times 10^4$) and Equivalent Isotropic Temperature Factors (Å^2) for [$Cp^{S2}{}_2Fe_2S_4$] (**2**)

Atom	x	y	z	B_{eq}[a)]
Fe(1)	2096.0(3)	2897.0(4)	4999.6(4)	2.9
Fe(2)	4827.8(3)	2765.6(3)	5809.9(4)	2.6
S(1)	3394.5(6)	3853.2(7)	6572.8(8)	3.7
S(2)	3677.5(6)	3489.8(7)	4717.4(9)	3.6
S(3)	2530.7(7)	1226.6(7)	4740.2(10)	4.1
S(4)	4091.7(7)	1157.3(7)	5200.7(10)	3.9
Si(1)	1144.0(10)	2223.2(14)	1789.0(11)	5.7
Si(2)	185.2(9)	2972.8(11)	7063.6(11)	4.6
Si(3)	6632.0(9)	1999.7(11)	3415.1(10)	4.4
Si(4)	5907.3(9)	2682.1(9)	8737.8(9)	4.0
C(1)	967(3)	2902(4)	3558(3)	4.2
C(2)	567(3)	2393(3)	4331(4)	4.0
C(3)	584(3)	3184(3)	5651(4)	3.9
C(4)	991(3)	4226(3)	5673(4)	4.1
C(5)	1212(3)	4062(3)	4439(4)	4.3
C(6)	6317(2)	2656(3)	5139(3)	3.5
C(7)	6302(2)	2120(3)	6015(3)	3.1
C(8)	6038(3)	3929(3)	7260(3)	3.4
C(9)	5932(3)	3997(3)	7134(4)	3.9
C(10)	4106(3)	3831(3)	5884(4)	3.8
C(11)	−53(4)	2522(6)	900(5)	6.9
C(12)	1266(7)	648(7)	1297(6)	10.6
C(13)	2347(5)	2876(9)	1474(6)	10.0
C(14)	−63(8)	1443(6)	6592(8)	10.9
C(15)	−1048(5)	3876(7)	7601(7)	9.1
C(16)	1247(5)	3540(8)	8403(6)	9.6
C(17)	7190(8)	556(6)	3052(7)	10.0
C(18)	5461(5)	1973(8)	2314(5)	9.1
C(19)	7676(5)	2926(6)	3252(7)	8.2
C(20)	6947(6)	3618(7)	10026(5)	9.7
C(21)	6174(9)	1167(6)	8340(6)	11.4
C(22)	4551(5)	3077(8)	9291(7)	9.7

a) The equivalent isotropic temperature factors for non-hydrogen atoms were computed using the following expression: $B_{eq}=4/3(B_{11}a^2+B_{22}b^2+B_{33}c^2+B_{12}ab\cos\gamma+B_{13}ac\cos\beta+B_{23}bc\cos\alpha)$. The B_{ij}'s are defined by $\exp[-(h^2B_{11}+k^2B_{22}+l^2B_{33}+2hkB_{12}+2hlB_{13}+2klB_{23})]$.

Table 7. Selected Interatomic Distances (Å) and Angles (°) for [$Cp^{S2}{}_2Fe_2S_4$] (**2**)

Fe(1)–Fe(2)	3.497(1)		
Fe(1)–S(1)	2.266(1)	Fe(1)–S(2)	2.252(1)
Fe(1)–S(3)	2.112(1)	Fe(2)–S(1)	2.265(1)
Fe(2)–S(2)	2.252(1)	Fe(2)–S(4)	2.105(1)
S(1)–S(2)	2.033(2)	S(3)–S(4)	1.997(1)
S(1)–Fe(1)–S(2)	53.48(3)	S(1)–Fe(1)–S(3)	97.95(4)
S(2)–Fe(1)–S(3)	98.32(4)	S(1)–Fe(2)–S(2)	53.50(4)
S(1)–Fe(2)–S(4)	97.92(3)	S(2)–Fe(2)–S(4)	98.17(4)
Fe(1)–S(1)–Fe(2)	101.03(4)	Fe(1)–S(1)–S(2)	62.90(5)
Fe(2)–S(1)–S(2)	62.93(5)	Fe(1)–S(2)–Fe(2)	101.87(5)
Fe(1)–S(2)–S(1)	63.61(5)	Fe(2)–S(2)–S(1)	63.57(5)
Fe(1)–S(3)–S(4)	110.56(5)	Fe(2)–S(4)–S(3)	111.12(5)

of [$Cp^{S2}{}_2Fe_2S_4$], [$Cp_2Fe_2S_4$], and [$Cp^*{}_2Fe_2S_4$] contains an end-on type S_2 and a side-on type S_2 ligands.

Two Cp^{S2} ligands in **2** are eclipsed, which is probably caused by the steric repulsion between $SiMe_3$ groups and disulfide ligands rather than that between $SiMe_3$ groups on the different Cp^{S2} ligands. The ring conformation is the same as that of [$Cp_2Fe_2S_4$], but different from that of [$Cp^*{}_2Fe_2S_4$] (*staggered*).

The Fe–Fe distance is 3.497(1) Å, indicating no Fe–Fe bonding interaction between them, and is comparable to those of [$Cp_2Fe_2S_4$] (3.494 Å)[19] and [$Cp^*{}_2Fe_2S_4$] (3.530 Å).[2] The Fe–S and the S–S distances around the S_2 ligands of **2** are also quite similar to those of [$Cp_2Fe_2S_4$] and [$Cp^*{}_2Fe_2S_4$].

This work was supported by Grants-in-Aid for Scientific Research Nos. 07240202 and 07216206 from the Ministry of Education, Science and Culture.

References

1) Abbreviations used in this paper: $Cp=C_5H_5$, $Cp^*=C_5Me_5$, $Cp^{S1}=C_5H_4(SiMe_3)$, $Cp^{S2}=1,3\text{-}C_5H_3(SiMe_3)_2$, $MeCp=C_5H_4Me$, $EtCp^*=C_5EtMe_4$, and Cp′=general expression for Cp and substituted cyclopentadienyl ligands.

2) H. Brunner, N. Janietz, W. Meier, G. Sergeson, J. Wachter, T. Zahn, and M. L. Ziegler, *Angew. Chem., Int. Ed. Engl.*, **24**, 1060 (1985).

3) R. A. Schunn, C. J. Fritchie, Jr., and C. T. Prewitt, *Inorg. Chem.*, **5**, 892 (1965).

4) P. J. Vergamini and G. J. Kubas, *Prog. Inorg. Chem.*, **21**, 261 (1976).

5) G. J. Kubas and P. J. Vergamini, *Inorg. Chem.*, **20**, 2667 (1981).

6) K. C. Frisch, *J. Am. Chem. Soc.*, **75**, 6050 (1953).

7) I. M. Pribytkova, A. V. Kisin, Yu. N. Luzikov, N. P. Makoveyeva, V. N. Torocheshnikov, and Yu. A. Ustynyuk, *J. Organomet. Chem.*, **30**, C57 (1971).

8) E. W. Abel and S. Moorhouse, *J. Organomet. Chem.*, **28**, 211 (1971).

9) G. A. Tolstikov, M. S. Miftakhov, and Y. B. Monakov, *Zh. Obshch. Khim.*, **46**, 1778 (1976).

10) J. Okuda and E. Herdtwerk, *J. Organomet. Chem.*, **373**, 99 (1989).

11) "International Tables for X-Ray Crystallography," Kynoch, Birmingham, England (1974), Vol. IV, Tables 2.2A and 2.3.1.

12) R. F. Stewart, E. R. Davidson, and W. T. Simpson, *J. Chem. Phys.*, **42**, 3175 (1965).

13) T. Sakurai and K. Kobayashi, *Rikagaku Kenkyusho Hokoku*, **55**, 69 (1979).

14) The UV-vis spectral data for [$Cp^*{}_2Fe_2S_4$]:[15] λ_{max} (ε) 771 (4400) and 464 (5200) nm.

15) S. Inomata, unpublished result.

16) H. L. Blonk, J. G. M. van der Linden, J. J. Steggerda, and J. Jordanov, *Inorg. Chim. Acta*, **158**, 239 (1989).

17) H. L. Blonk, J. Mesman, J. G. M. van der Linden, J. J. Steggerda, J. M. M. Smits, G. Beurskens, P. T. Beurskens, C. Tonon, and J. Jordanov, *Inorg. Chem.*, **31**, 962 (1992).

18) a) S. Inomata, H. Tobita, and H. Ogino, *Inorg. Chem.*, **30**, 3039 (1991); b) H. Brunner, A. Merz, J. Pfauntsch, O. Serhadli, J. Wachter, and M. L. Ziegler, *Inorg. Chem.*, **27**, 2055 (1988).

19) a) H. Chanaud, A. M. Ducourant, and C. Giannotti, *J. Organomet. Chem.*, **190**, 201 (1980); b) R. Weberg, R. C. Haltiwanger, and M. R. DuBois, *Organometallics*, **4**, 1315 (1985).

20) V. A. Uchtman and L. F. Dahl, *J. Am. Chem. Soc.*, **91**, 3756 (1969).
21) H. Behm, J. Jordanov, F. G. Moers, and P. T. Beurskens, *J. Crystallogr. Spectrosc. Res.*, **21**, 741 (1991).
22) T. B. Rauchfuss, D. P. S. Rodgers, and S. R. Wilson, *J. Am. Chem. Soc.*, **108**, 3114 (1986).
23) A. Müller, W. Jaegermann, and J. H. Enemark, *Coord. Chem. Rev.*, **46**, 245 (1982).